Catalysis Letters (2019) 149:965–973
https://doi.org/10.1007/s10562-019-02672-3

The Effect of SO_2 and H_2O on the Interaction Between Pt and TiO_2(P-25) During Catalytic CO Oxidation

Kenji Taira[1,2] · **Hisahiro Einaga**[1]

Received: 8 October 2018 / Accepted: 11 January 2019 / Published online: 29 January 2019

Abstract

The deactivation of noble metal catalysts by SO_2 and H_2O is a common issue in the post combustion treatment of flue gases from sintering processes in the steel industry. In an effort to develop SO_2-tolerant CO-oxidation catalysts, herein, we investigated the effect of SO_2 and H_2O on the catalytic activity of Pt/TiO_2(P-25) catalysts for CO oxidation using X-ray photoelectron spectroscopy (XPS), transmission electron microscopy (TEM), and diffuse-reflectance infrared Fourier-transform (DRIFT) spectroscopy. Pt/TiO_2(P-25) catalysts, in the absence of SO_2 and presence of H_2O, enhanced the activity and stability of CO oxidation, while being largely suppressed and irreversibly deactivated in the presences of SO_2. The XPS and TEM results suggested that variations in the Pt particle size and oxidation state were not major causes of the deactivation. Instead, according to DRIFT spectra, the interaction between CO and H_2O at the metal-support interface was weakened after the formation of $TiOSO_4$ on the TiO_2 surface in the presence of SO_2. This resulted in a loss of the previously observed enhancement of CO oxidation under humid conditions. These results indicate that in the presence of SO_2, the formation of $TiOSO_4$ is the major cause of irreversible deactivation. Therefore, removal of the $TiOSO_4$ layer from the TiO_2 surface is a crucial step for catalyst regeneration.

Graphical Abstract

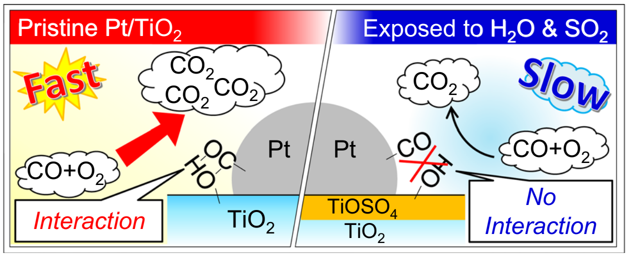

Keywords Catalyst regeneration · CO oxidation · Platinum catalyst · SO_2 · TiO_2

1 Introduction

TiO_2 is frequently used as a supporting material for metal and metal oxide catalysts due to its high surface area, strong metal-support interactions, and chemical stability [1]. These properties also make TiO_2-supported metal or metal oxide catalysts promising for applications such as those related to the production of fine chemicals and catalytic CO oxidation. Among supporting materials for noble metal catalysts, TiO_2-supported Pt (Pt/TiO_2) catalysts showed higher activity for CO oxidation than other supported Pt catalysts (e.g., Pt/

Electronic supplementary material The online version of this article (https://doi.org/10.1007/s10562-019-02672-3) contains supplementary material, which is available to authorized users.

✉ Kenji Taira
taira.e84.kenji@jp.nssmc.com

[1] Department of Material Sciences, Faculty of Engineering Sciences, Kyushu University, Kasuga, Fukuoka 816-8580, Japan

[2] Advanced Technology Research Laboratories, Nippon Steel & Sumitomo Metal Corporation, 20-1 Shintomi, Futtsu, Chiba 293-8511, Japan

SiO_2) due to the interaction between Pt and the TiO_2 support [2].

One useful feature of TiO_2 is its robustness against SO_2, which is often present in reaction gases. Several studies reported that Pt/TiO_2 catalysts have an advantage over other supporting materials in the tolerance of SO_2 [3–7]. Indeed, the effect of SO_2 on the activity and stability of Pt/TiO_2 catalysts under dry gas conditions has been established. However, in the real world setting, a high concentration of H_2O coexists with SO_2 in many flue gases [8]. Reportedly, every sintering plant in the steel industry emits ~ 1 million Nm^3/h of flue gas, from which ~ 1% represents CO, 20–200 ppm SO_2, and 10–20% H_2O [9]. Considering the hazardous properties of CO, removing this gas by catalytic oxidation under the influence of SO_2 and H_2O would be highly desirable. Under oxidative conditions, SO_2 is oxidized and reacts with H_2O to form H_2SO_4 [7].

In a previous study, we have found that the formation and build-up of H_2SO_4 on the Pt/TiO_2 catalyst surface leads to a further catalyst deactivation [7]. Usually, reactants diffuse through the inter-particle spacing inside the Pt/TiO_2 particle agglomerates. However, these inter-particle mesopores could be blocked by H_2SO_4. Notably, the blocking can be removed at temperatures above 300 °C, thereby making catalyst deactivation due to pore blocking by H_2SO_4 reversible. Although using TiO_2 supports containing larger mesopores reduces the need for reactivation, the catalytic activity of Pt/TiO_2 is not completely recovered after H_2SO_4 removal, thus suggesting the presence of additional deactivation mechanisms. It is, therefore, necessary to determine other origins of catalytic deactivation to further improve the Pt/TiO_2 catalyst stability under reaction conditions that may be encountered in the real world.

Herein, we employ TiO_2(P-25) as the supporting material for Pt to investigate the origin of catalytic deactivation under the influence of SO_2 and H_2O. Our previous report showed that Pt/TiO_2(P-25) had large mesopores and exhibited high stability during CO oxidation using a gas mixture containing both SO_2 and H_2O [7]. Furthermore, TiO_2(P-25) is advantageous for its high purity and absence of sulfuric impurities [10], which allows a detailed discussion on the effect of SO_2 on the catalyst. In this study, the effect of SO_2 and H_2O on Pt/TiO_2(P-25) during the reaction is discussed using X-ray photoelectron spectroscopy (XPS) and diffuse-reflectance infrared Fourier-transform (DRIFT) spectroscopy. The effect of H_2O on CO oxidation related to the Pt/TiO_2(P-25) catalytic activity was first investigated, followed by the effect of both H_2O and SO_2, in order to clarify the poisoning effect of SO_2 in detail.

2 Experimental

2.1 Catalyst Preparation

The Pt/TiO_2(P-25) catalysts were prepared by the impregnation method. An aqueous solution of $H_2PtCl_6 \cdot 6H_2O$ (Sigma-Aldrich, > 99.995%) was added dropwise to TiO_2 (Catalysis Society of Japan (CSJ), JRC-TIO-4 (identical to Degussa P-25)) [11]. The samples were then dried at 110 °C overnight and calcined at 500 °C for 1 h. The supports were dried at 110 °C for 10 h and subsequently heated at 500 °C in air for 1 h before use. The catalyst with 0.1 wt% Pt (based on the amount of precursor used) was denoted as Pt/TiO_2(P-25). Additionally, the catalyst employed in the XPS and DRIFT measurements was prepared in the same manner, with 1 wt% Pt, and was denoted as Pt1/TiO_2(P-25).

2.2 Catalyst Characterization

The surface area of the catalysts was determined by the Brunauer–Emmett–Teller (BET) method from the N_2 adsorption isotherm measured by an adsorption measurement instrument (Japan BEL, BEL-max). X-ray diffraction (XRD) measurements were performed for all of the prepared catalysts using an XRD instrument (Rigaku, RINT-TTR III). The ratio between the anatase and rutile phases in TiO_2 was determined following previously reported protocols [7, 12]. The results from both the BET and XRD measurements were in accord with those obtained previously [7] (Table S1).

TEM images of the Pt/TiO_2(P-25) catalysts were obtained using a transmission electron microscope (FEI, Tecnai G2) in order to determine the dispersion of Pt. All images were obtained as bright-field images. The accelerating voltage was adjusted to 200 kV, and the average Pt particle size was determined using the procedure described in the Supporting Information of our previous paper [7]. The size distribution of Pt nanoparticles was determined using TEM images (Figs. S1 and S2).

The oxidation states of Pt in Pt1/TiO_2(P-25) and the amount of S were estimated by XPS. All spectra were obtained using an XPS analyzer (ULVAC-Phi, Quantum-2000) equipped with a monochromated Al X-ray source and charge neutralizer. All measurements were performed at a pass energy of 29.35 eV and recording step of 0.125 eV. The peak shift derived from the charge build up in the catalysts was corrected by adjusting the binding energy of the C 1*s* peak to 285.0 eV. Additionally, we recorded Ti 2*p* and O 1*s* spectra in order to assess the validity of the adjustment. The deviation of the peak maxima between the catalysts was confirmed to be below 0.2 eV. All XPS spectra were fitted using Gaussian–Lorentzian symmetric peak shapes and an iterative Shirley background. The peak area ratio followed the prediction from quantum mechanics, and the ratio between Pt $4f_{7/2}$ and Pt $4f_{5/2}$ was adjusted to 4:3 for all pairs of Pt $4f$ peaks. The difference in binding energy between Pt $4f_{7/2}$ and Pt $4f_{5/2}$ was adjusted to 3.33 ± 0.03 eV. TiO_2(P-25) supports without Pt were also characterized by XPS (Fig. S3), and the observed broad peaks were in the fitting of the Pt1/TiO_2(P-25) XPS spectra.

The CO adsorption state on Pt was elucidated by DRIFT spectroscopy. The Pt/TiO_2(P-25) catalyst was collected from the tube reactor and placed in the in situ DRIFT cell equipped with ZnSe windows. DRIFT spectra were recorded using an infrared spectrometer (is50, Thermo Fisher Scientific) equipped with a mercury cadmium telluride (MCT) detector. The reflectance spectra were obtained at 30 °C with a resolution of 4 cm^{-1} and were transformed to the Kubelka–Munk function. All samples were subjected to Ar flow for 10 min to remove excess water, followed by 5% CO/He gas until the peak intensity remained constant. CO was then purged by Ar flow for 5 min before beginning the measurements. In addition, the amount of SO_4^{2-} species on the catalysts in the samples following the test reactions with SO_2 was examined by DRIFT. The measurements were performed under H_2 flow at a heating rate of 5 °C/min.

2.3 Catalytic Test Reactions

The catalytic activity of the Pt/TiO_2(P-25) catalyst was evaluated by CO oxidation ($CO + 1/2O_2 \rightarrow CO_2$) at atmospheric pressure with the same apparatus described elsewhere [7]. A reduction pretreatment using H_2 was performed at 500 °C for 30 min before each test reaction. Under humid test reaction conditions of CO oxidation without SO_2, the gas composition was 1% CO, 10% O_2, and 20% H_2O, and 69% N_2. For CO oxidation with SO_2 under humid conditions, the gas composition was 1% CO, 10% O_2, 20% H_2O, 40 ppm SO_2, and 40 ppm NO, with N_2 making up the remainder. The gas composition under dry reaction conditions was 1% CO, 10% O_2, and 89% N_2. The reaction gas compositions were set according to the actual exhaust gas composition of the sintering plant of Nippon Steel & Sumitomo Metal Corporation. The total gas flow was adjusted to 100 cm^3/min and the space velocity (SV) was adjusted to 6,000,000 cm^3/h/gcat. Notably, at such high SV, the amount of catalyst is too small, i.e. 1.0 mg, to ensure its contact with the gas flow. Therefore, the catalysts were mixed with TiO_2 powder to increase the catalyst bed thickness. The total amount of the sample in the catalyst bed was adjusted to 30 mg. Typically, the reactions were performed at 250 °C for 5–20 h. The gas composition of the outlet gas from the reactor was determined with an infrared gas analyzer (Yokogawa Electric, IR-200) and conversion of CO was calculated using the CO and CO_2 concentrations. Test reactions confirmed that bare TiO_2 exhibited almost no activity for CO oxidation (Fig. S4), indicating that the catalytic properties of Pt/TiO_2 are determined by the Pt particles and the Pt–TiO_2 interface. The catalyst with 1 wt% Pt (Pt1/TiO_2(P-25)) was also subjected to the same reaction conditions before the XPS measurements and DRIFT studies. The Pt-size distribution and CO-oxidation activity were similar for 0.1 wt%- and 1.0 wt%-Pt/TiO_2(P-25) catalysts (Figs. S2 and S5), confirming that the chemical condition was similar for these catalysts.

3 Results and Discussion

3.1 Effect of H_2O on the CO Oxidation Reaction in the Absence of SO_2

To understand the effect of H_2O on the catalytic activity of Pt/TiO_2(P-25) toward CO oxidation, the reaction was first performed in the absence of SO_2. The time course profiles of the CO oxidation in the presence of catalyst Pt/TiO_2(P-25) and the absence of SO_2 at 250 °C differ under dry and humid conditions, as well as whether reduced with H_2 (pretreatment) or left untreated (Fig. 1). While, under dry conditions, both the reduced and untreated catalyst led to the decrease in CO conversion over time, the pretreated catalyst decreased to a lesser extent. In contrast, under humid conditions, both the untreated and reduced Pt/TiO_2(P-25) catalysts exhibited

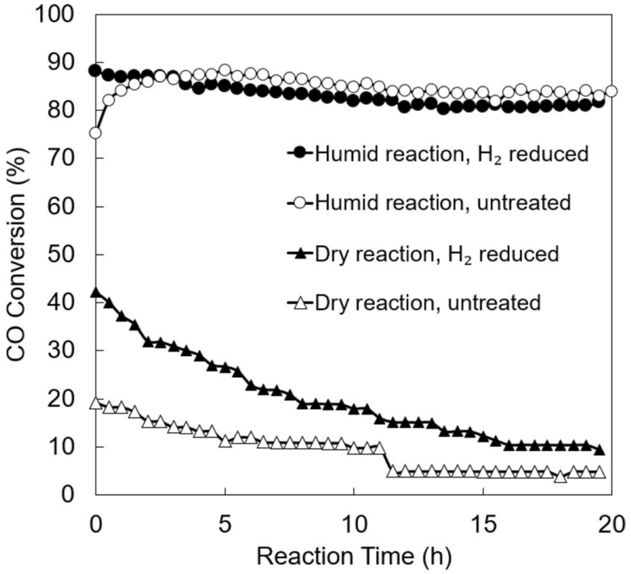

Fig. 1 CO oxidation reaction test results without SO_2. Gas composition, dry: 1% CO, 10% O_2, 0% H_2O, 89% N_2; Gas composition, humid: 1% CO, 10% O_2, 20% H_2O, 79% N_2; SV: 6,000,000 cm^3/h/gcat

comparable and stable activity for CO oxidation throughout the reaction. These results indicate that the presence of water vapor accelerated and stabilized the CO oxidation of Pt/TiO_2(P-25), irrespective of the pretreatment conditions.

As described above, water vapor in the reaction gas improved the activity and stability of the Pt/TiO_2(P-25) catalyst for CO oxidation. In order to understand the origin of these results, the catalysts were characterized by XPS and TEM. XPS spectra before and after the test reactions are shown in Fig. 2. The results of XPS are summarized in Table 1. Clear differences are observed after the test reactions for the catalysts both with and without H_2 reduction. In the untreated catalyst prior to the test reaction, Pt was comprised solely of Pt^{2+} and Pt^{4+} (no Pt^0) species. The Pt species were then reduced during the test reaction, resulting in a decrease in the Pt^{2+} and Pt^{4+} species and increase in metallic Pt^0. In the pretreated (reduced) catalyst, the Pt species were mainly Pt^0 with a small amount of Pt^{2+}(no Pt^{4+}). After the test reaction, the amount of Pt^0 species slightly decreased, while that of Pt^{2+} increased. These results suggest that the oxidation state of Pt on TiO_2(P-25) during the CO oxidation under dry conditions is affected by the interaction between the metal and TiO_2(P-25) support. CO oxidation of the oxidized Pt^{2+} or Pt^{4+} sites was slower than that of the reduced Pt^0 sites under dry conditions [13]. The higher activity of the reduced Pt/TiO_2(P-25) was ascribed to the larger amount of Pt^0 species, which represent the active sites for CO oxidation under dry conditions.

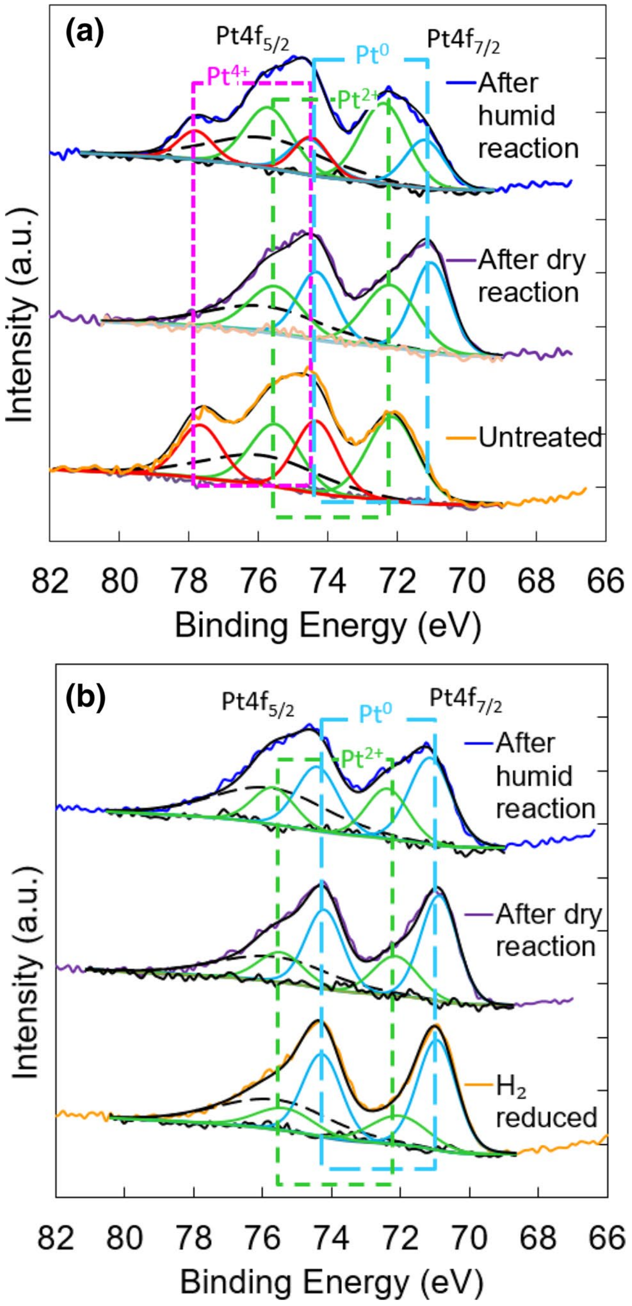

Fig. 2 XPS spectra (Pt 4*f*) of Pt1/TiO_2(P-25) after CO oxidation under dry and humid reaction conditions **a** without (untreated) and **b** with H_2 reduction pretreatment

Table 1 Pt oxidation states and ratios in Pt1/TiO_2(P-25) before and after the test reaction under dry and humid conditions without SO_2

	Pt^0	Pt^{2+}	Pt^{4+}
Untreated			
After humid reaction	0.27	0.53	0.20
After dry reaction	0.51	0.49	0
Before reaction	0	0.57	0.43
H_2 reduced			
After humid reaction	0.63	0.37	0
After dry reaction	0.69	0.31	0
Before reaction	0.72	0.28	0

All values were calculated from the peak areas in Fig. 2

The oxidation state of Pt also changed after CO oxidation under humid conditions. The ratio of Pt^{2+}/Pt^0 species in the pretreated (reduced) Pt/TiO_2(P-25) catalyst increased after CO oxidation in the presence of water vapor, indicating that the Pt sites on TiO_2(P-25) were oxidized. Conversely, as for untreated Pt/TiO_2(P-25), the fraction of Pt^{4+} and Pt^{2+} decreased and Pt^0 was formed after the reaction. For both catalysts, the fraction of oxidized Pt species (Pt^{2+} and Pt^{4+}) after the CO oxidation under humid conditions was larger than that under dry conditions. In marked contrast to CO oxidation under dry conditions, no clear relationship between the fraction of reduced Pt^0 sites and CO oxidation activity of Pt/TiO_2 catalysts could be determined.

TEM results also indicate the strong interaction between Pt and the TiO_2 support. The average diameters of Pt particles on the TiO_2 supports are listed in Table 2. The average Pt size before the reaction was ~ 1.4 nm and remained almost unchanged when the Pt loading increased from 0.1 to

Table 2 Pt particle diameter determined by TEM measurement of catalysts before and after the reactions under humid conditions with and without SO_2

	Pt size (nm)	
	0.1 wt% Pt	1.0 wt% Pt
After reaction without SO_2		
H_2 reduced	1.90	1.95
Untreated	1.73	1.69
After reaction with SO_2		
H_2 reduced	2.61	2.72
Before the reaction	1.47	1.41

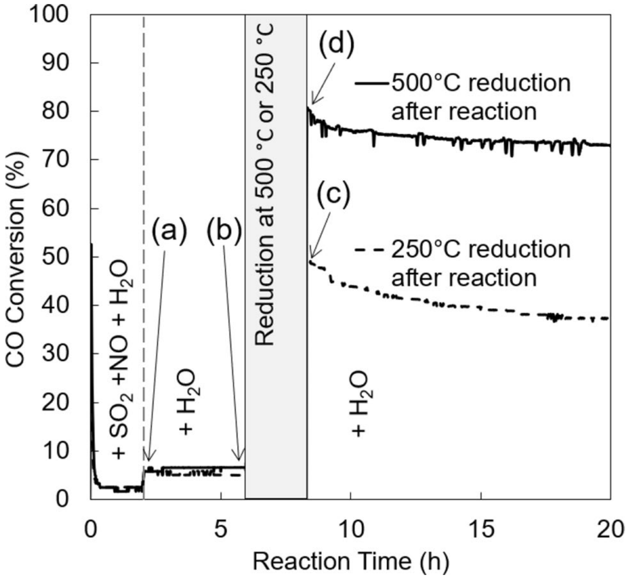

Fig. 3 CO oxidation reaction test with SO_2. The catalysts were reduced in H_2 flow at 500 °C. Gas composition: 1% CO, 10% O_2, 20% H_2O, SO_2, NO 40 or 0 ppm, N_2 remaining balance; SV: 6,000,000 cm^3/h/gcat. The samples for XPS and DRIFT studies were obtained at the corresponding reaction times indicated by symbols: (a) after 2-h reaction in the presence of SO_2 and H_2O, (b) after subsequent 4-h reaction under humid condition without SO_2, (c) after H_2 reduction at 250 °C subsequent to the reaction, and (d) after H_2 reduction at 500 °C subsequent to the reaction

1.0 wt%. The particle size distribution is also similar (Fig. S1). In addition, Pt particles were smaller than 2 nm even after the test reactions. This result also supports the idea that the interaction between Pt particles and the TiO_2(P-25) support is strong enough to stabilize the Pt particles consisting of < 200 Pt atoms [14].

3.2 CO Oxidation Reaction with SO_2

The effect of SO_2 on the catalytic CO oxidation was assessed by a test reaction (Fig. 3). The reaction conditions were identical to those described earlier in Sect. 3.1, but now the reaction also included SO_2. Before the test reaction, the catalysts were reduced under H_2 flow at 500 °C. Notably, the catalysts were almost instantly deactivated under the reaction conditions containing SO_2. Previous reports show that the adsorption of SO_2 on the Pt surface causes catalytic deactivation [15]. Additionally, our previous study indicated that the by-product H_2SO_4 resulted in pore blocking and deceleration of the oxidation process [7]. For these reasons, lower catalytic activity in the presence of SO_2 was observed, but catalytic CO oxidation could be partly restored by the removal of H_2SO_4. Herein, we have discussed several causes of deactivation originating from SO_2.

The reversible deactivation and reactivation were confirmed by the subsequent SO_2-free reaction. CO conversion increased around 2 h after the removal of SO_2 from the reaction gas (Fig. 3). However, the obtained conversion in that case was much lower than when the catalyst was not exposed to SO_2 at all (Fig. 1). This result suggests that the adsorption of SO_2 in the presence of H_2O also irreversibly deactivated the Pt/TiO_2(P-25) catalysts. To verify the effect of irreversible deactivation, H_2 reduction treatment at 500 °C or 250 °C was subsequently carried out. In the case of H_2 reduction at 500 °C, the catalytic activity was recovered to the same level as when no SO_2 was present (Fig. 1). In contrast, H_2 reduction at 250 °C restored the catalytic activity by only half of what was attained with treatment at 500 °C. This result suggests that the causes of the irreversible deactivation were almost fully removed by H_2 reduction at 500 °C, but not at 250 °C.

3.3 Causes of Irreversible Deactivation of Pt/TiO_2(P-25) in the Presence of SO_2 and H_2O

Pt/TiO_2(P-25) catalysts were reversibly and irreversibly deactivated when SO_2 was present in the reaction gas (Fig. 3). Irreversible deactivation was mostly recovered by H_2 reduction treatment at 500 °C, but only partly by reduction at 250 °C. Below, we have discussed the origin of irreversible deactivation of Pt/TiO_2(P-25) in the presence of SO_2 and H_2O related to four possible causes, ultimately showing that the alteration of the interaction between Pt and TiO_2(P-25) is a major cause of the irreversible deactivation of Pt/TiO_2(P-25) in the presence of SO_2.

The first possible cause of irreversible deactivation is the formation of Pt sulfate species. In the presence of SO_2, the Pt/TiO_2(P-25) catalysts were subjected to oxidative conditions. It is known that Pd is deactivated when it transforms to Pd sulfate species [16, 17]. A similar transformation could conceivably occur with Pt, which is why we verified the chemical state of Pt in the Pt1/TiO_2(P-25) catalyst after the reaction using XPS measurements (Fig. 4). The oxidation state of Pt and ratios between the oxidation states

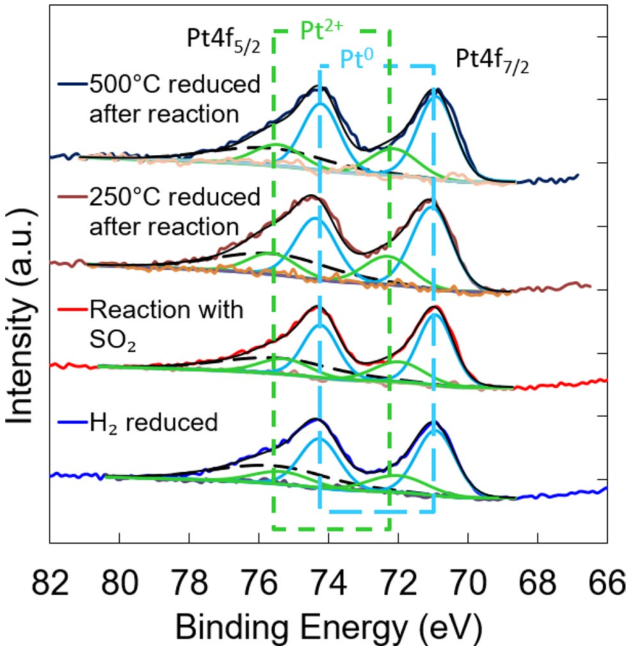

Fig. 4 XPS spectra (Pt 4*f*) of Pt1/TiO_2(P-25) after the CO oxidation with SO_2

Table 3 Oxidation states of Pt and their ratios in Pt1/TiO_2(P-25) before and after the test reaction with SO_2

	Pt^0	Pt^{2+}	Pt^{4+}
Reaction without SO_2			
After reaction	0.63	0.37	0
Reaction with SO_2			
500 °C reduced after reaction	0.71	0.29	0
250 °C reduced after reaction	0.71	0.29	0
After reaction	0.71	0.29	0
Before reaction			
500 °C reduced	0.72	0.28	0

All values were calculated from the peak areas in Fig. 4

are described in Table 3. As can be seen, most Pt remained metallic (Pt^0) even after the test reaction with SO_2; almost no difference was observed before and after CO oxidation with SO_2. In addition, the ratio remained almost identical even after the reduction treatment at 250 °C and 500 °C (Table 3). These results suggest that the alteration of the chemical state of Pt is not the origin of the deactivation during the reaction in the presence of SO_2. It is noteworthy that Pt was more oxidized after the reaction test without SO_2 (Fig. 2) than after the reaction with SO_2 (Fig. 4). As previously discussed (Sect. 3.1), Pt was oxidized during the reaction test without SO_2 due to the interaction between Pt and the TiO_2(P-25) support. Therefore, XPS results suggest that the interaction between Pt and TiO_2(P-25) was moderated by SO_2.

The second possible cause of irreversible deactivation is the sintering of Pt particles during the reaction. Reportedly, the sintering of Pt is accelerated by SO_2 [15, 18]. Previous studies even show the formation of H_2SO_4 and $TiOSO_4$ as by-products during the reactions containing both SO_2 and H_2O [7, 19, 20]. The formation of strong acid, H_2SO_4, can further promote the sintering of Pt during the reaction, which may cause irreversible deactivation of the catalysts. To assess the effect of the sintering, the average diameter of Pt particles was determined by TEM measurements of the catalysts before and after the reaction. The results are summarized in Table 2. The average size of the Pt particles on TiO_2(P-25) almost doubled following the reaction with SO_2. This result indicates that the sintering of Pt at least partly caused the irreversible deactivation of the Pt/TiO_2(P-25) catalysts during the reactions in the presence of SO_2. However, the deactivation cannot be fully attributed to the sintering of Pt for two reasons: (1) the size of Pt after the reaction and (2) the catalytic activity after H_2 reduction treatment following the reaction. While the size of Pt particles almost doubled after the reaction, the increase was only ~40% compared to the result obtained after the reaction without SO_2. It is unreasonable to attribute the drastic deactivation observed to such a small increase in the Pt particle size (Fig. 3). This conclusion was also supported by the high activity of Pt/TiO_2(P-25) after the H_2 reduction treatment following the reaction with SO_2. If the major cause of Pt/TiO_2(P-25) deactivation was the sintering of Pt particles, the catalytic activity could not be recovered by such a simple reduction treatment. Combined, these results suggest that the sintering of Pt was a minor cause of the irreversible deactivation of Pt/TiO_2(P-25) catalysts during the reactions with SO_2.

The third possible cause of irreversible deactivation is the coverage of Pt particles by SO_x species. Adsorbed SO_x species on Pt prevent CO oxidation on the Pt surface, which leads to lower Pt/TiO_2(P-25) activity. We found that the physical adsorption of SO_x species is not a major source for the irreversible deactivation of Pt/TiO_2(P-25). It has been reported that SO_x species on Pt are oxidized and transferred from the Pt surface to the surface of the oxide supports during reactions in an oxidative atmosphere at temperatures > 200 °C [21]. Furthermore, our previous report confirms the appearance of H_2SO_4 under reaction conditions identical to the aforementioned ones (Sects. 3.1 and 3.2), which also indicates the fast removal of SO_x species from the Pt surface [7]. For further assessment, we performed a DRIFT study to understand the CO adsorption on the Pt particles (Fig. 5). An intense peak of CO adsorbed on metallic Pt^0, as well as a small peak of CO on Pt^{2+} was observed even after the reaction with SO_2 (Figs. 3a, b, 5a, b). In fact, the intensity of the main peak was comparable to those of the peaks before the test reaction (Fig. 5), thereby signifying that CO adsorbed on the Pt surface was not disturbed by the

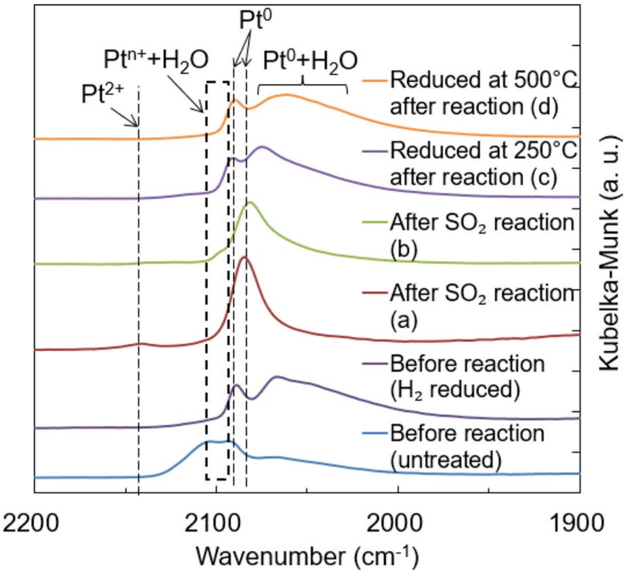

Fig. 5 DRIFT spectra of Pt1/TiO_2. The samples indicated by symbols (a)–(d) were collected at the corresponding reaction times reported in Fig. 3: (a) after 2-h reaction in the presence of SO_2 and H_2O, (b) after subsequent 4-h reaction under humid condition without SO_2, (c) after H_2 reduction at 250 °C subsequent to the reaction, and (d) after H_2 reduction at 500 °C to the reaction. All measurements were performed at room temperature. 5% CO/Ar gas flowed for 5 min after Ar purge. Then, CO gas was purged by Ar for 5 min before the measurement. Peaks were assigned according to a previous report [24]

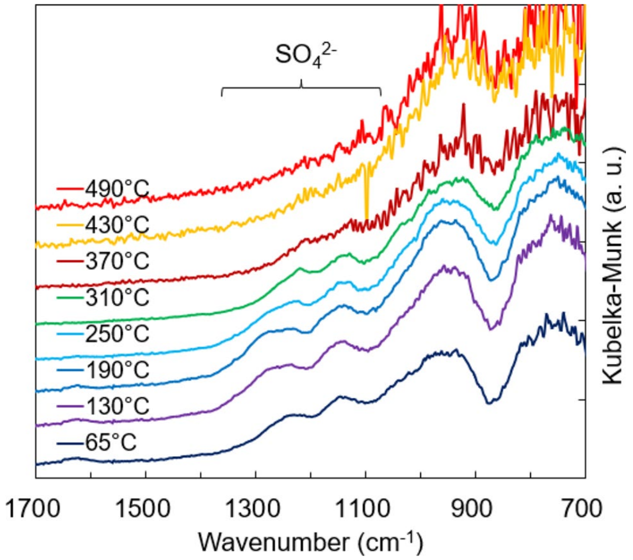

Fig. 6 DRIFT spectra obtained during heating under H_2 atmosphere after the test reaction with SO_2. The heating rate was 5 °C/min, with the spectra being recorded every 15 °C. Peaks ~ 1100–1300 cm^{-1} correspond to sulfate species [7, 15]

SO_x species present. This result also supports the conclusion that although the presence of SO_x species on the Pt surface is the cause for reversible catalytic deactivation, it is not a major cause for irreversible deactivation.

The fourth possible cause of irreversible deactivation of Pt/TiO_2(P-25) catalysts is the alteration of the interaction between Pt and the TiO_2(P-25) supports. As confirmed by XPS and DRIFT studies after the reaction (Figs. S6 and S7), SO_2 was oxidized on Pt–SO_4^{2-} species. Thermogravimetric analysis confirmed the formation of ~ 0.2 nm thick $TiOSO_4$ layer on all over the TiO_2 surface after the reaction in the presence of SO_2 (Fig. S8; Tables S2 and S3). This modification of the TiO_2 surface would alter the interaction between Pt and the TiO_2(P-25) supports. Several reports suggest that CO and H_2O form an intermediate state at the Pt-support interface, which leads to faster CO oxidation [22, 23]. The coverage of a TiO_2 surface by $TiOSO_4$ can therefore hinder the reaction between CO and H_2O at the Pt–TiO_2(P-25) interface. This would lead to a weaker enhancement of the CO oxidation by H_2O and, as a result, slower CO oxidation. This assumption is supported by the DRIFT spectra in Fig. 5. Clear differences are represented among the spectra. Although the adsorbed CO species are observed in all spectra, peaks corresponding to CO interacting with H_2O are absent only in the spectrum of Pt/TiO_2(P-25) after the reaction with SO_2 (Fig. 5a, b) [24]. This result suggests that CO does not interact with H_2O at Pt–TiO_2 interface on the TiO_2(P-25) support covered by $TiOSO_4$. This assumption is supported by the dependence of the peak intensity on the reduction temperature after the reaction test with SO_2. When reduction treatment was carried out at 500 °C after the reaction with SO_2, the peak intensity of CO interacting with H_2O on Pt^0 is stronger than that after the reduction treatment at 250 °C (Fig. 5c, d). As illustrated in the DRIFT spectra obtained during heating under H_2 atmosphere, the peaks of the SO_4^{2-} species weaken as the temperature is increased [7, 15, 25] (Fig. 6). No clear peaks of SO_4^{2-} species are observed at 490 °C, but weak peaks are confirmed at 250 °C. XPS spectra of S 2*p* are also in accordance with these results; the peak for SO_4^{2-} weakened after the reduction treatment following the test reaction (Fig. 7). These results suggest that the existence of SO_4^{2-} species on TiO_2(P-25) and $TiOSO_4$ weakened the interaction between CO and H_2O at Pt–TiO_2 interface, which led to the irreversible deactivation of Pt/TiO_2(P-25).

DRIFT studies suggest that the appearance of $TiOSO_4$ alter the interaction between H_2O and CO, which results in a weaker enhancement of the CO oxidation from H_2O and, thus, slower CO oxidation. In order to confirm this hypothesis, we performed CO oxidations under different conditions. CO oxidation in the presence of SO_2 was followed by CO oxidation under humid conditions without SO_2, and then by CO oxidation under dry reaction conditions without SO_2 (Fig. 8). It is worth noting that the CO conversion rate remained almost constant even after the removal of water, thereby indicating that the CO conversion rate was

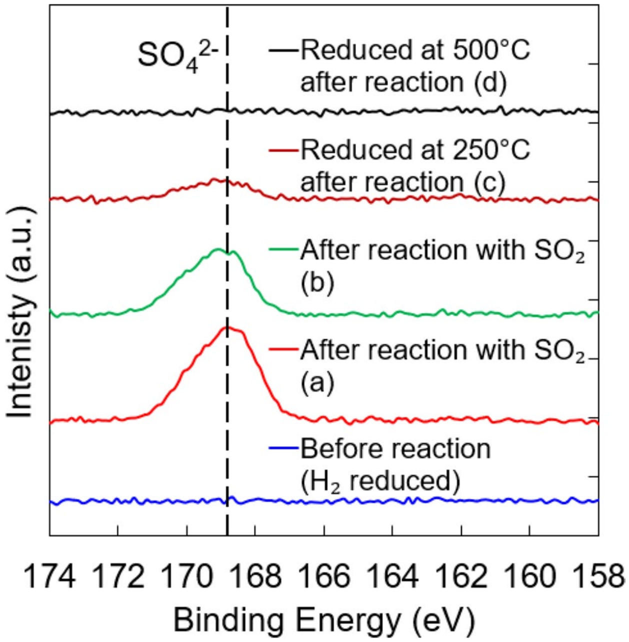

Fig. 7 XPS spectra (S 2*p*) of Pt1/TiO_2(P-25) before and after the CO oxidation with SO_2. The samples indicated by symbols (a)–(d) were collected at the corresponding reaction times indicated in Fig. 3: (a) after 2-h reaction in the presence of SO_2 and H_2O, (b) after subsequent 4-h reaction under humid condition without SO_2, (c) after H_2 reduction at 250 °C subsequent to the reaction, and (d) after H_2 reduction at 500 °C to the reaction

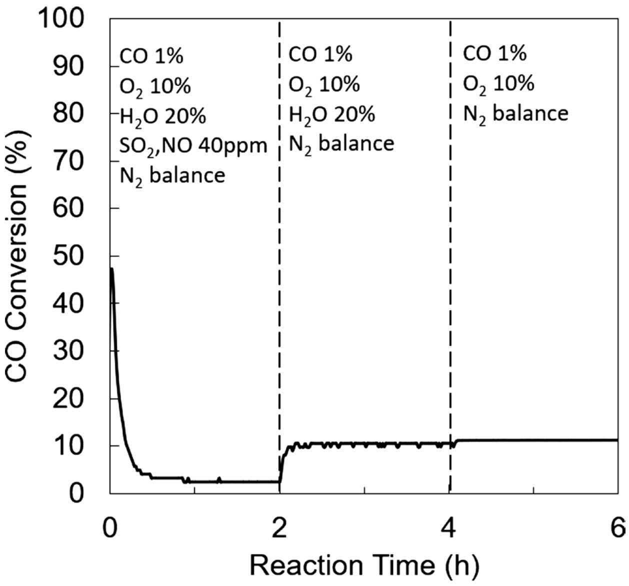

Fig. 8 CO oxidation test reaction with SO_2. The catalysts were reduced under H_2 flow at 500 °C. Gas composition: 1% CO, 10% O_2, 0% or 20% H_2O, 0 ppm or 40 ppm SO_2 and NO, N_2 remaining balance; SV: 6,000,000 cm^3/h/gcat

not affected by the presence of H_2O. These results indicate that there was no enhancement of the CO oxidation from H_2O after the reaction with SO_2, which clearly supports the idea that the coverage of TiO_2(P-25) with $TiOSO_4$ causes the irreversible deactivation of Pt/TiO_2(P-25) catalysts.

Taken together, all experimental results suggest that a $TiOSO_4$ layer coats TiO_2 surface, thus weakening the interaction between H_2O and CO at the Pt–TiO_2 interface and rendering the previously observed enhancement of CO oxidation from H_2O inactive. This suggests that removal of $TiOSO_4$ from the TiO_2(P-25) support is a crucial step in the catalyst regeneration. An easy approach to remove $TiOSO_4$ is heating the catalysts in reductive atmospheres. Reportedly, sulfate species decompose at lower temperature under a reductive rather than oxidative atmosphere [26]. Therefore, applying a reductive atmosphere enables the removal of $TiOSO_4$ at lower temperature while also avoiding the sintering of Pt on the support. Another possible approach is washing the catalysts with solvents that dissolve $TiOSO_4$ (e.g., water) in order to effectively regenerate the catalysts. Furthermore, the findings of this study also suggest another strategy to improving the SO_2 tolerance of the catalysts, namely modification of the TiO_2 surface with dopants. In particular, TiO_2 is known for its wide range of dopant options [27–29]. We expect that the thermal stability of the $TiOSO_4$ layer on the TiO_2 surface would be altered by dopants because the stability of sulfates strongly depends on the element type [26]. In addition, finer tuning of the chemical composition of the TiO_2 supports would possibly lead to a higher SO_2 tolerance of the Pt/TiO_2 catalysts.

4 Conclusions

In this study, we discussed the origin of irreversible deactivation of Pt/TiO_2(P-25) in relation to the presence of SO_2. Results from XPS and TEM measurements suggest that the oxidation state and size variation of Pt are not major causes of deactivation. In addition, DRIFT studies show that the interaction between CO and H_2O was weakened after the formation of $TiOSO_4$ on the TiO_2(P-25) surfaces. Furthermore, CO oxidation test reactions elucidated the absence of CO oxidation enhancement from H_2O in the presence of H_2O and SO_2, which results in a lower catalytic activity. Based on the results in this work, we concluded that the formation of $TiOSO_4$ is the major cause of irreversible deactivation after the reaction with SO_2. Therefore, the removal of $TiOSO_4$ is a crucial step to reactivating the catalysts after the reactions with gas mixtures containing SO_2 and H_2O.

Acknowledgements This research did not receive any specific grant from funding agencies in the public, commercial, or not-for-profit sectors.

References

1. Bagheri S, Muhd Julkapli N, Bee Abd Hamid S (2014) Titanium dioxide as a catalyst support in heterogeneous catalysis. Sci World J. https://doi.org/10.1155/2014/727496
2. Kimura K, Einaga H, Teraoka Y (2011) Preparation of highly dispersed platinum catalysts on various oxides by using polymer-protected nanoparticles. Catal Today 164:88–91. https://doi.org/10.1016/j.cattod.2010.10.006
3. Matsumoto S, Ikeda Y, Suzuki H et al (2000) NOx storage-reduction catalyst for automotive exhaust with improved tolerance against sulfur poisoning. Appl Catal B Environ 25:115–124. https://doi.org/10.1016/S0926-3373(99)00124-1
4. Irfan MF, Goo JH, Kim SD, Hong SC (2007) Effect of CO on NO oxidation over platinum based catalysts for hybrid fast SCR process. Chemosphere 66:54–59. https://doi.org/10.1016/j.chemosphere.2006.05.044
5. Hirata H, Hachisuka I, Ikeda Y et al (2001) NOx storage-reduction three-way catalyst with improved sulfur tolerance. Top Catal 16:145–149. https://doi.org/10.1023/A:1016603502952
6. Xue E, Seshan K, Ross JRH (1996) Roles of supports, Pt loading and Pt dispersion in the oxidation of NO to NO_2 and of SO_2 to SO_3. Appl Catal B Environ 11:65–79. https://doi.org/10.1016/S0926-3373(96)00034-3
7. Taira K, Nakao K, Suzuki K, Einaga H (2016) SO_x tolerant Pt/TiO_2 catalysts for CO oxidation and the effect of TiO_2 supports on catalytic activity. Environ Sci Technol 50:9773–9780. https://doi.org/10.1021/acs.est.6b01652
8. Mowery DL, McCormick RL (2001) Deactivation of alumina supported and unsupported PdO methane oxidation catalyst: the effect of water on sulfate poisoning. Appl Catal B Environ 34:287–297. https://doi.org/10.1016/S0926-3373(01)00222-3
9. Lu L, Ooi TC, Li X (2015) Sintering emissions and their mitigation technologies. In: Liming L (ed) Iron ore, 1st edn. Woodhead Publishing, Cambridge, pp 551–579
10. Ohno T, Sarukawa K, Tokieda K, Matsumura M (2001) Morphology of a TiO_2 photocatalyst (Degussa, P-25) consisting of anatase and rutile crystalline phases. J Catal 203:82–86. https://doi.org/10.1006/jcat.2001.3316
11. Matsuhashi H (2011) Manual for reference catalysts, 5th edn. Japan Catalyst Society, Tokyo
12. Depero LE, Sangaletti L, Allieri B et al (1998) Niobium-titanium oxide powders obtained by laser-induced synthesis: microstructure and structure evolution from diffraction data. J Mater Res 13:1644–1649. https://doi.org/10.1557/JMR.1998.0226
13. Kimura K, Einaga H, Teraoka Y (2010) Catalytic properties of platinum supported on titanium dioxide by liquid-phase adsorption of colloidal nanoparticles. Catal Lett 139:72–76. https://doi.org/10.1007/s10562-010-0388-y
14. Lentz C, Jand SP, Melke J et al (2017) DRIFTS study of CO adsorption on Pt nanoparticles supported by DFT calculations. J Mol Catal A Chem 426:1–9. https://doi.org/10.1016/j.molcata.2016.10.002
15. Wakita H, Kani Y, Ukai K et al (2005) Effect of SO_2 and H_2S on CO preferential oxidation in H_2-rich gas over Ru/Al_2O_3 and Pt/ Al_2O_3 catalysts. Appl Catal A Gen 283:53–61. https://doi.org/10.1016/j.apcata.2004.12.035
16. Sharma HN, Sharma V, Hamzehlouyan T et al (2014) SOx oxidation kinetics on Pt(111) and Pd(111): first-principles computations meet microkinetic modeling. J Phys Chem C 118:6934–6940. https://doi.org/10.1021/jp501538v
17. Mowery DL, Graboski MS, Ohno TR, McCormick RL (1999) Deactivation of PdO–Al_2O_3 oxidation catalyst in lean-burn natural gas engine exhaust: aged catalyst characterization and studies of poisoning by H_2O and SO_2. Appl Catal B Environ 21:157–169. https://doi.org/10.1016/S0926-3373(99)00017-X
18. Auvray XP, Olsson L (2013) Sulfur dioxide exposure: a way to improve the oxidation catalyst performance. Ind Eng Chem Res 52:14556–14566. https://doi.org/10.1021/ie402153u
19. Kröcher O, Widmer M, Elsener M, Rothe D (2009) Adsorption and desorption of SO_x on diesel oxidation catalysts. Ind Eng Chem Res 48:9847–9857. https://doi.org/10.1021/ie900882p
20. Neyestanaki AK, Klingstedt F, Salmi T, Murzin DY (2004) Deactivation of postcombustion catalysts, a review. Fuel 83:395–408. https://doi.org/10.1016/j.fuel.2003.09.002
21. Smirnov MY, Kalinkin AV, Pashis AV et al (2014) Interaction of SO_2 with Pt model supported catalysts studied by XPS. J Phys Chem C 118:22120–22135. https://doi.org/10.1021/jp5069126
22. Rajasree R, Hoebink JHBJ, Schouten JC (2004) Transient kinetics of carbon monoxide oxidation by oxygen over supported palladium/ceria/zirconia three-way catalysts in the absence and presence of water and carbon dioxide. J Catal 223:36–43. https://doi.org/10.1016/j.jcat.2003.12.014
23. Manasilp A, Gulari E (2002) Selective CO oxidation over Pt/alumina catalysts for fuel cell applications. Appl Catal B Environ 37:17–25. https://doi.org/10.1016/S0926-3373(01)00319-8
24. Hadjiivanov KI (1998) IR study of CO and H_2O coadsorption on Pt^{n+}/TiO_2 and Pt/TiO_2 samples. J Chem Soc Faraday Trans 94:1901–1904. https://doi.org/10.1039/a801892h
25. Şentürk GS, Vovk EI, Zaikovskii VI et al (2012) SOx uptake and release properties of TiO_2/Al_2O_3 and BaO/TiO_2/Al_2O_3 mixed oxide systems as NOx storage materials. Catal Today 184:54–71. https://doi.org/10.1016/j.cattod.2011.12.006
26. Habashi F, Mikhail SA, Van KV (1976) Reduction of sulfates by hydrogen. Can J Chem 54:3646–3650. https://doi.org/10.1139/v76-524
27. Pan CJ, Tsai MC, Su WN et al (2017) Tuning/exploiting strong metal-support interaction (SMSI) in heterogeneous catalysis. J Taiwan Inst Chem Eng 74:154–186. https://doi.org/10.1016/j.jtice.2017.02.012
28. Hanaor DAH, Sorrell CC (2011) Review of the anatase to rutile phase transformation. J Mater Sci 46:855–874. https://doi.org/10.1007/s10853-010-5113-0
29. McFarland EW, Metiu H (2013) Catalysis by doped oxides. Chem Rev 113:4391–4427. https://doi.org/10.1021/cr300418s